energies

Article

Innovative Single-Day Installation Vessel for Offshore Wind Turbines

Moo-Sung Ryu [1,*], Sang-Ryul Kim [2], Dong-Ho Cho [3] and Joon-Goo Kang [4]

[1] Renewable Energy Group, Korea Electric Power Corporation Research Institute (KEPRI), Daejeon 34056, Korea
[2] Department of System Dynamics, Korea Institute of Machinery and Materials (KIMM), Daejeon 34056, Korea; srkim@kimm.re.kr
[3] Renewable Energy Laboratory, Korea Electric Power Corporation Research Institute (KEPRI), Daejeon 34056, Korea; dh.cho@kepco.co.kr
[4] SM Instruments, Daejeon 34141, Korea; jgkang@smins.co.kr
* Correspondence: faust001@kepco.co.kr; Tel.: +82-42-865-5321

Abstract: Transportation and installation of a wind turbine system is one of the main factors for business availability of offshore wind power due to its high cost and technical difficulty. The purpose of this study is to develop an innovative transportation and installation method for offshore wind turbines. We refer to this installation process as an All-In-One-Installation (A.I.O.I), and the special vessel used is referred to as a multipurpose mobile base (MMB). In this study, the short-range transportation and penetration and pull-out tests of the entire wind turbine system are performed before field demonstration. All the offshore wind turbine systems were transported and installed safely at one time. Field demonstration was conducted on the installation site approximately 15 km from the harbor in approximately 5 h using the suction method. In the actual A.I.O.I demonstration test, stable values were obtained. The respective changes in inclination at the center of the MMB and the tower were within 0.1° and 0.2° during operation, respectively, because of the reduction of longitudinal and transverse sway of the MMB induced by the self-weight assembly and ballast. The presented method constitutes an innovative transportation and installation method useful for the offshore wind power industry demonstrating single-day installation feasibility. This installation method can be used to configure the fleet in the development of large-scale offshore wind farms, but it is also possible to install turbines in individual units for research or small businesses. With minor A-Frame modifications, it can be applied as a multipurpose vessel to maintain the blades or heavy components, or can be used for pile driving, or for the lifting/installation of offshore structures.

Keywords: offshore wind power; suction bucket; all-in-one installation; multipurpose mobile base; lifting trunnion; clamping device; pitch angle; overturning

check for updates

Citation: Ryu, M.-S.; Kim, S.-R.; Cho, D.-H.; Kang, J.-G. Innovative Single-Day Installation Vessel for Offshore Wind Turbines. *Energies* **2022**, *15*, 3914. https://doi.org/10.3390/en15113914

Academic Editor: Madjid Karimirad

Received: 26 April 2022
Accepted: 24 May 2022
Published: 25 May 2022

1. Introduction

As shown in Figure 1, global offshore wind power installation is increasing annually, and its total capacity will be 57.2 GW by the end of 2021; it also constitutes a renewable energy source that is expected to be developed continuously in the future, and it is evaluated currently as the strongest alternative to achieve carbon neutrality on a worldwide scale [1].

In addition, offshore wind power is capable of being developed for large-scale power source development and is a renewable energy source with high technological perfection and reliability. As shown in Figure 2, the levelized cost of energy (LCOE) has decreased by approximately 48% over a ten-year period, and in the case of Europe, it can be observed that it has reached the level of grid parity.

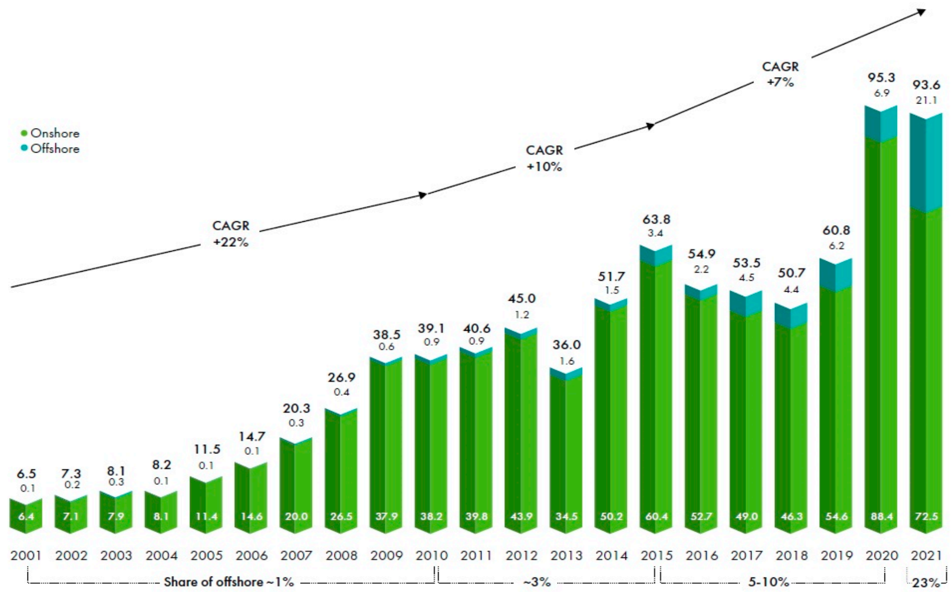

Figure 1. Historic development of total installations of wind power (source: Global wind report 2022, Global Wind Energy Council).

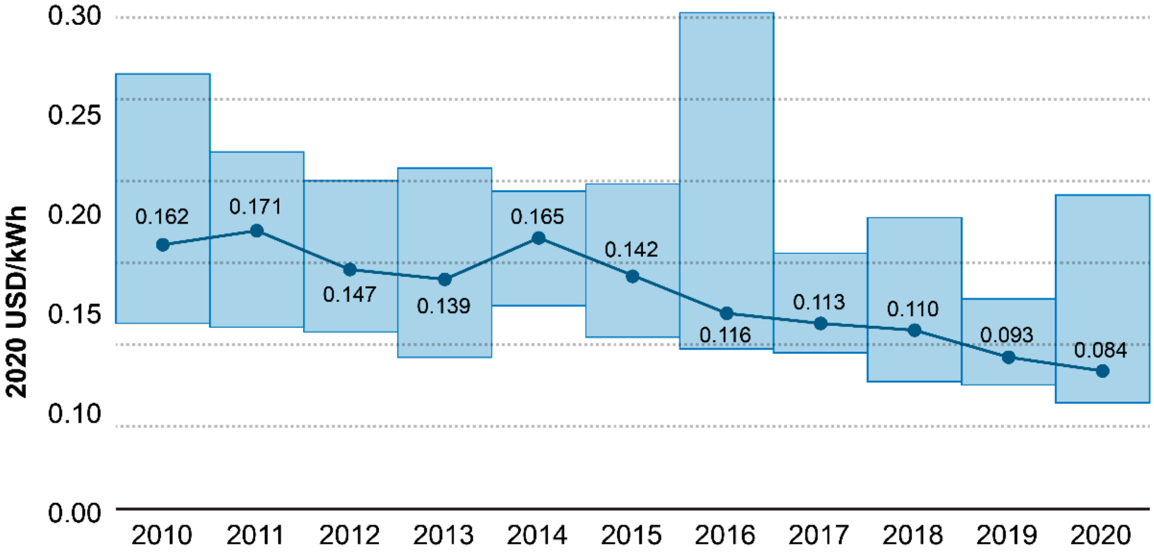

Figure 2. Weighted average LCOE of offshore wind during the period of 2010–2020 (source: Offshore renewables: An action agenda for deployment, International Renewable Energy Agency).

There are several main factors that affect the offshore wind power LCOE. Currently, the locations of the developed wind farms are gradually expanding to far offshore and, as shown in Figure 3, the water depth of the installed sea area is very important. It can be observed that the support structure, and transportation and installation technology has a direct influence on the total cost of a wind farm [2]. Accordingly, the Korean Electric Power Corporation Research Institute (KEPRI), which started as a research project of a new concept offshore wind power support structure in 2014, developed into a suction bucket foundation to install offshore wind turbines using only the weight and water pressure difference between the inner and outer piles, and demonstrated it onsite. Additionally, in previous studies, an evaluation method for its stability was suggested [3–5].

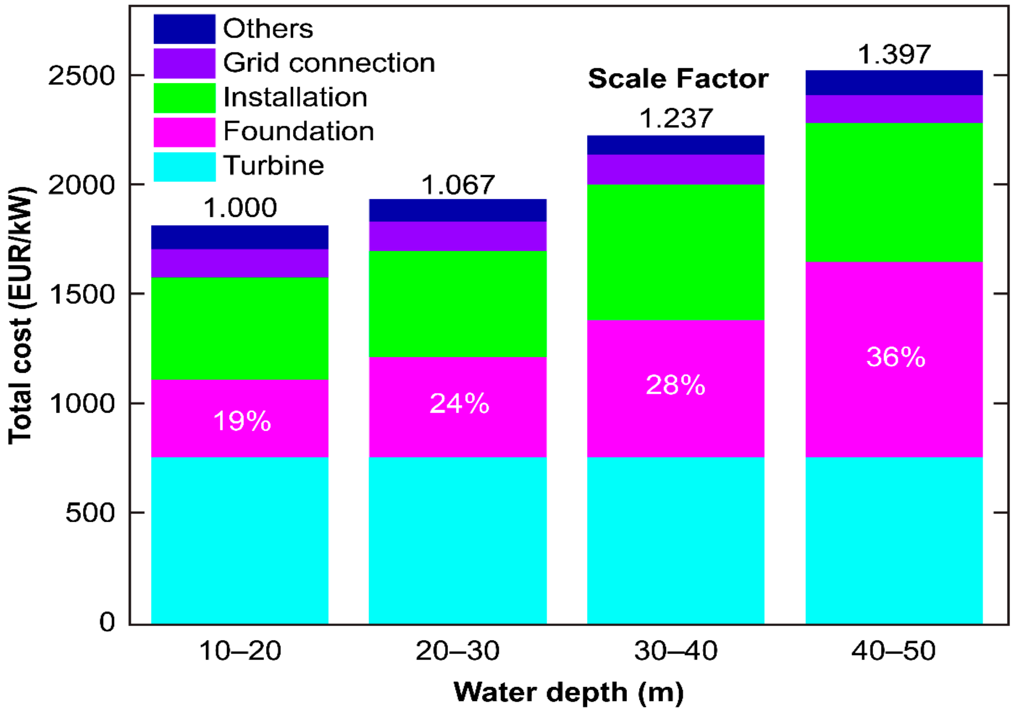

Figure 3. Cost effect of water depth for offshore wind farm development (source: Technical Report No 6, European Environment Agency, 2009).

Over the course of this research project, KEPRI observed the technical characteristics of the suction bucket foundation that can be separated from the seabed ground, combined it with an offshore wind turbine to assemble the entire system at the port, and then developed a new technical solution that allows lifting, transportation, and installation within a single day. In 2016, the multipurpose mobile base (MMB) research project was initiated. At that time in Europe, which has a mature offshore wind power market, offshore wind turbine installation by a wind turbine installation vessel was a common practice. As a result, there was a supply market (separate dedicated fleets for each business stage and business purpose as shown in Figure 4) in the transportation and installation field [6].

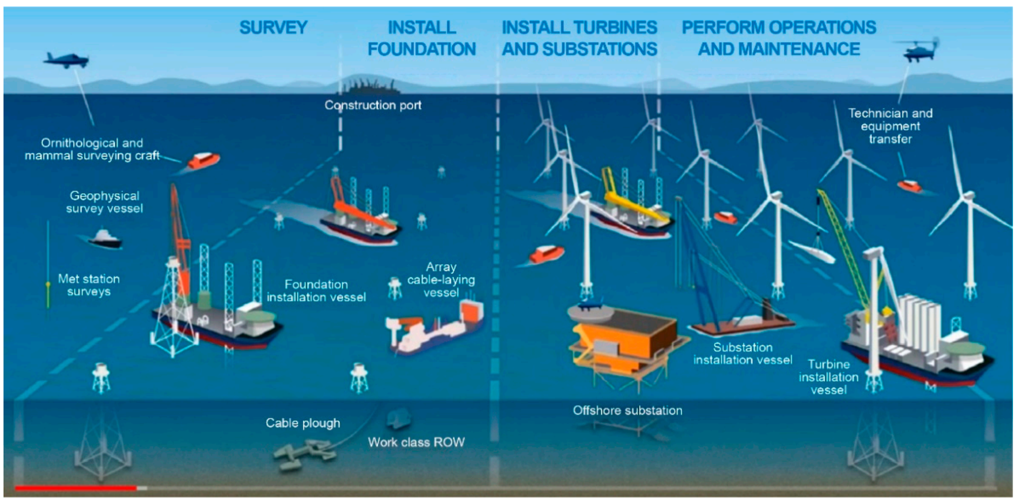

Figure 4. Various offshore vessels used for dedicated purposes at each construction stage (source: Clean Energy Group, Webinar 2019).

In contrast, in Korea, where the offshore wind power installation market was in the early stages, there were no dedicated installation vessels, and the installation of offshore wind turbines or support structures also operated in a non-standardized manner using a combined fleet with onshore cranes mounted on jack-up barges. As shown in Figure 5, Korea's offshore wind power construction market has developed at a very slow rate compared with Europe, and the construction business has been stagnant, with a cumulative installed capacity of 98 M as of 2019 [7]. For this reason, there was almost no demand for offshore wind power installation vessels in 2016 at the onset of this research project, and the direction of technology development was limited regarding the improvement of the existing jack-up barges or crane capacity.

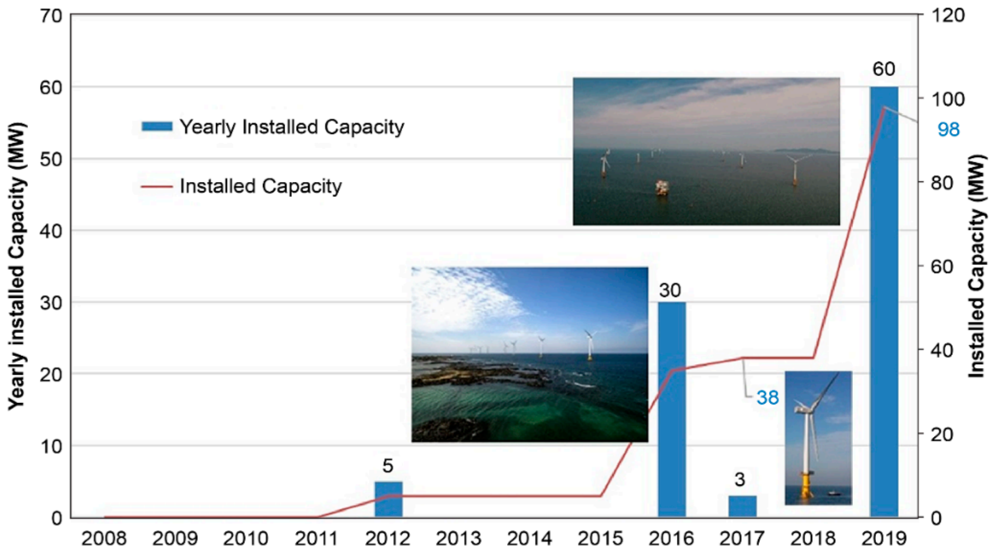

Figure 5. Offshore wind power development in Korea (No records in 2020–2021, Data source: Korea Wind Energy Association, 2020).

However, due to the Korean government's policy drive of renewable energy 3020, the newly installed capacity target for wind power was set at 16.5 GW for 2030. As a result, large-scale offshore wind farm development promotion plans were announced within a very short time period, led by local governments and the private sector. Accordingly, the KEPRI started this study to develop an all-in-one-installation (A.I.O.I), a new concept of offshore wind turbine transportation and installation method that can actively cope with large-scale developments in the future, encompassing the small-scale offshore wind farm development market.

2. Basic Design and Safety Analysis

2.1. Basic Concept of Multipurpose Mobile Base

Offshore wind power is directly affected by marine weather conditions, such as high wave heights, strong currents, and typhoons because the wind farm is built in the open sea far from the coast. Accordingly, large amounts of funds and time are invested in transporting and installing the support structures and wind turbines. Accidents or delays due to bad weather during these major processes constitute very important factors that determine the success or failure of the entire project. The MMB, a special offshore wind turbine installation vessel, is a new concept for the safe installation of wind turbines regardless of the marine weather conditions. After assembling the wind turbine and support structure in the harbor, the wind turbine can be installed in the sea in a single day by using the suction method to lift the entire pre-assembled wind power system and transport it to the installation point by sea, as shown in Figure 6.

Figure 6. Basic concept of Multi-purpose Mobile Base.

To lift the entire pre-assembled wind power system at once, the lower foundation must be separated from the ground; this action is performed by the suction bucket. As shown in Figure 7, the suction bucket uses only the water pressure difference inside and outside the pile and its own weight as a driving force, which occurs when a large steel pipe is mounted on the sea floor and then discharged using the suction pump installed on the top of the pile, as the pile penetrates the seabed. It is an ecofriendly construction method that uses only the hydraulic pressure difference. Thus, there is almost no noise and vibration, and there are no floating particles during pile driving. The verticality of tripod suction pile is controlled by suction pump operation, which means that each pump operates separately according to its pile penetration depth to balance the three feet. Operators should be very attentive when securing the level of each pile during this process. Another technical challenge for A.I.O.I is the weight and height of the wind turbine system. As the offshore wind turbine is a heavy-weight-extra-long structure, a large crane with a large lifting capacity is required to lift it safely. Additionally, it is necessary to design a hull that controls longitudinal and lateral sway to prevent damage caused by overturning or falling during transportation and thus, enabling stable operation. KEPRI did not apply the jack-up and rotating crane adopted by European offshore wind turbine installation vessels but reduced the hull manufacturing cost dramatically (by 20 times) based on the use of a floating barge-based A-Frame and lifting wire. Since the center of gravity (CG) of the offshore wind turbine is relatively high compared to other structures, the CG of the entire system combined with the lower support structure is located on the wind turbine tower. However, in general, the wind turbine tower is not sufficiently strong to attach the lifting connection (trunion). Therefore, the lifting wires are connected to the lower support structure, below the CG of the entire system, and the wind turbine sway is controlled through the hydraulic clamping system on the upper part of the A-frame. Based on this method, even if the capacity and height of the turbine are increased, the size of the vessel can be minimized, thereby securing applicability to large-capacity turbines.

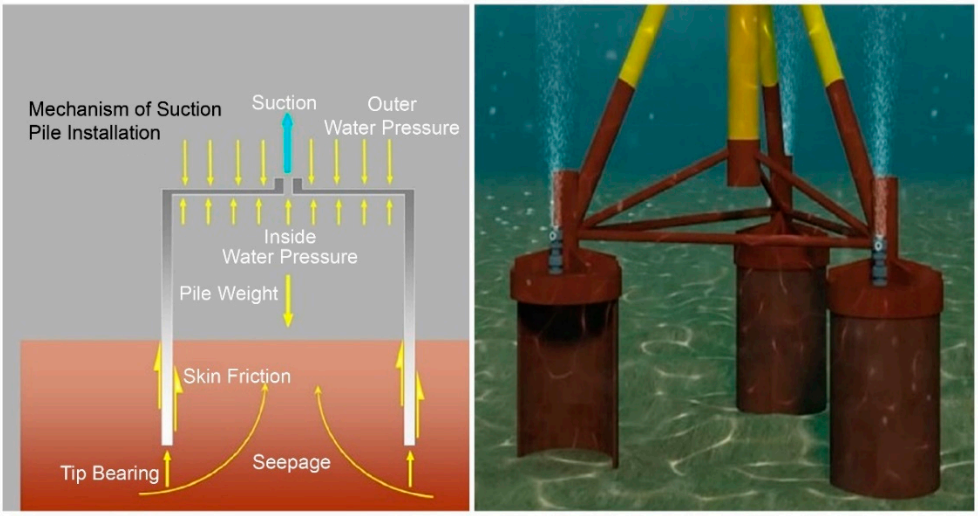

Figure 7. Installation of suction pile foundation.

2.2. System Definition and Basic Assumptions

As described in Section 2.1, the wind turbine system is connected to the A-frame on the MMB with lifting wires and is fixed with a hydraulic device on the upper part of the A-frame. In addition, given that the wind turbine system is transported while seated on the support beam, it can be assumed that the behavior of the wind turbine is the same as that of the MMB when it sails on the sea. However, in the case of hoisting the wind turbine in the port to mount it on the MMB, or when the wind turbine is lifted down from the MMB to settle it on the seabed after being transported to the installation location, the wind turbine is connected only with lifting wires and moves like a pendulum. To evaluate the safety of the behavior of the wind turbine during this process, an analytical approach is adopted. It is simplified and analyzed as a two-dimensional problem based on considerations of the MMB operation procedure and the physics of pendulum motion. For convenience, the following are assumed:

1. The wind turbine is a rigid rod that is reduced to a point mass at the CG.
2. The wind turbine is connected to the two points of the fixed MMB frame at the same height as the wires.
3. The initial angle between the wire and the wind turbine structure is constant.
4. The attachment between the wire and the wind turbine are assumed to be an ideal hinge (moment-free).
5. During operation, the wire length does not increase as a function of the load.
6. The hydraulic fixing device on the upper part of the A-frame acts as a rotational and horizontal stiffness for the wind turbine.
7. The wire system for fixing the lower part acts as a horizontal stiffness.
8. The wind turbine is initially in equilibrium (vertical upright).
9. The change in the angle of the wire is very small.

Figure 8 shows a schematic of the system for the wind turbine behavior analysis and the variables used in the analysis. In the figure, the point P_{CG} is the CG of the wind turbine, and P_a and P_b are the wire connection points. P_c is the position at the upper hydraulic fixing device, k_θ is the rotational stiffness, and k_{xc} is the horizontal stiffness. P_l is the point at which the horizontal stiffness of the lower fixing wire system k_{xl} acts. The angles of the wires with respect to the vertical axis are θ_a and θ_b, and the angles change by θ_1 and θ_2 at the equilibrium angles $\overline{\theta}_a$ and $\overline{\theta}_b$, respectively. θ_{wt} represents an angle at which the wind turbine is inclined from the vertical axis.

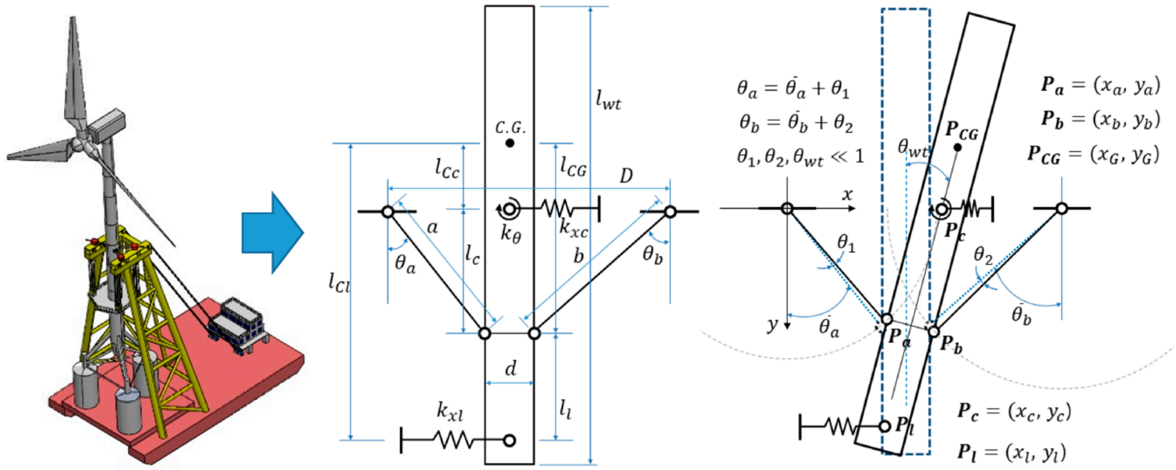

Figure 8. Simple two-dimensional model of an on-board wind turbine system.

2.3. System Analysis

First, to examine the behavior of a wind turbine connected with two wires as shown in Figure 9, consider the case in which it is connected only with wires without the upper and lower fixing devices. If the wire length and the connection angle are all the same, the wind turbine can be modeled simply as a rod whose CG is above the extended intersection point of the two wires (the point O), as shown in Figure 9.

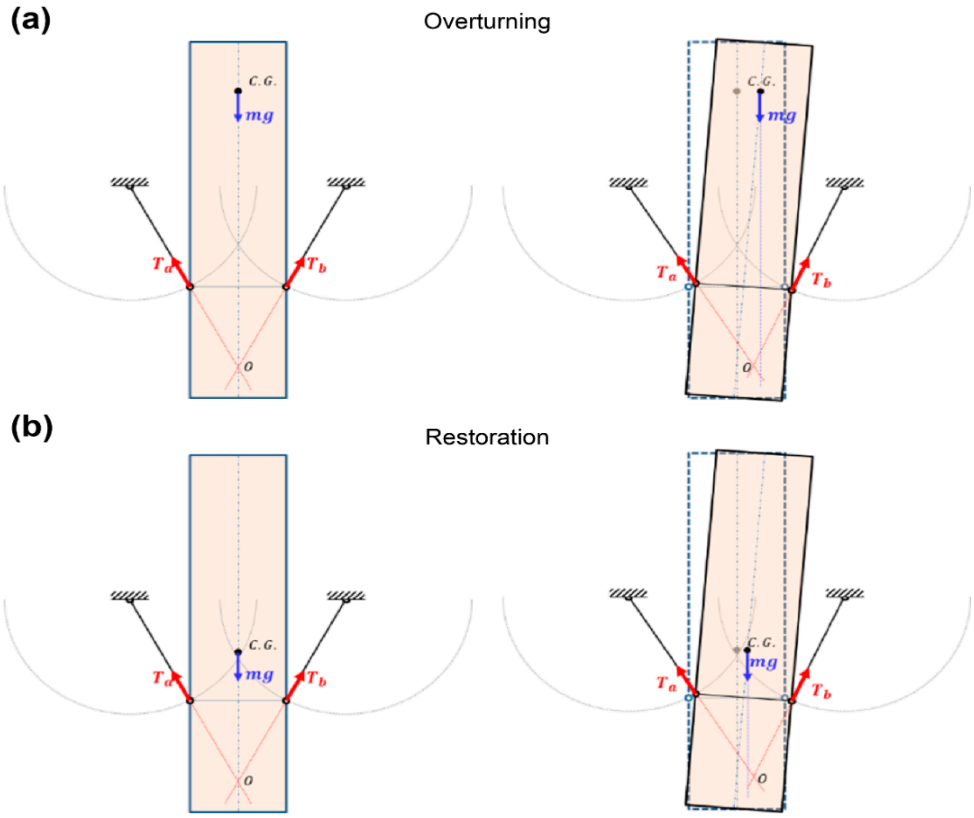

Figure 9. Free-body diagram of a simplified wind turbine.

As shown in Figure 9a, when the perpendicular line drawn from the CG of the wind turbine deviates to the right of the extended intersection point of two wires (the point O) after the wind turbine rotates in equilibrium, the wind turbine rotates further in the same direction and eventually overturns. Conversely, if the perpendicular line drawn from the

CG point is to the left of the point O, as shown in Figure 9b, the wind turbine undergoes a pendulum motion that returns to its original position with the force (moment) of restitution caused by its own weight in the opposite direction of the rotation. It is possible to induce a condition for this pendulum motion.

Figure 10 summarizes the equations of motion in each direction for the generalized model of the wind turbine shown in Figure 8.

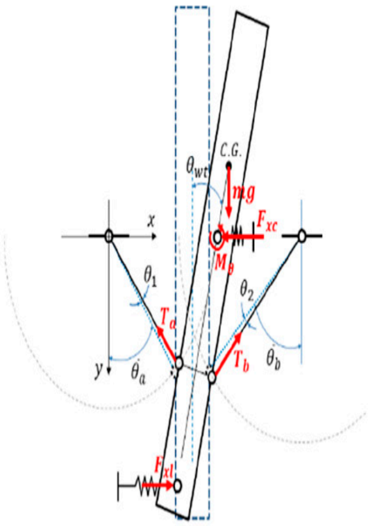

$$\sum F_x = m\dot{x}_G$$

$$-T_a\frac{\bar{x}_a + x_1}{a} + T_b\frac{D - \bar{x}_b - x_1}{b} - \left\{(k_{xc} + k_{xl}) + (k_{xc}l_c - k_{xl}l_l)\frac{\tan\bar{\theta}_a + \tan\bar{\theta}_b}{d}\right\}x_1 = m\left\{1 + \frac{l_{CG}(\tan\bar{\theta}_a + \tan\bar{\theta}_b))}{d}\right\}\ddot{x}_1$$

$$\sum F_y = m\dot{y}_G$$

$$-T_a\frac{\bar{y}_a - x_1\tan\bar{\theta}_a}{a} - T_b\frac{\bar{y}_a + x_1\tan\bar{\theta}_b}{b} + mg = m\left(\frac{-\tan\bar{\theta}_a + \tan\bar{\theta}_b}{2}\right)\ddot{x}_1$$

$$\sum M = I\dot{\theta}_{wt}$$

$$T_a\left[\frac{l_{CG}\bar{x}_a}{a} + \frac{d\bar{y}_a}{2a} + \left\{\frac{l_{CG}}{a} + \frac{l_{CG}\bar{y}_a}{ad}(\tan\bar{\theta}_a + \tan\bar{\theta}_b) - \frac{d\tan\bar{\theta}_a}{2a} - \frac{\bar{x}_a}{2a}(\tan\bar{\theta}_a + \tan\bar{\theta}_b)\right\}x_1\right]$$
$$-T_b\left[\frac{D - \bar{x}_b}{b}l_{CG} + \frac{d\bar{y}_a}{2b} - \left\{\frac{l_{CG}}{b} + \frac{l_{CG}\bar{y}_a}{bd}(\tan\bar{\theta}_a + \tan\bar{\theta}_b) - \frac{d\tan\bar{\theta}_b}{2b} - \frac{D - \bar{x}_b}{2b}(\tan\bar{\theta}_a + \tan\bar{\theta}_b)\right\}x_1\right]$$
$$-\frac{k_\theta(\tan\bar{\theta}_a + \tan\bar{\theta}_b)}{d}x_1 + k_{xc}l_{Cc}\left(1 + l_c\frac{\tan\bar{\theta}_a + \tan\bar{\theta}_b}{d}\right)x_1 + k_{xl}l_{Cl}\left(1 - l_l\frac{\tan\bar{\theta}_a + \tan\bar{\theta}_b}{d}\right)x_1 = I_{CG}\frac{\tan\bar{\theta}_a + \tan\bar{\theta}_b}{d}\ddot{x}_1$$

Figure 10. Equations of motion for the on-board wind turbine system.

In the case in which the initial angles are the same ($\bar{\theta}_a = \bar{\theta}_b \neq 0$) and the wires shown in Figure 9 have the same lengths ($a = b$), the natural frequency of the pendulum can be derived as follows.

$$\omega^2 = mg\left\{-l_{CG} + \frac{d^2}{4a\cos\bar{\theta}_a}\left(\frac{1}{\tan^2\bar{\theta}_a} + 1\right) + \frac{d\tan\bar{\theta}_a}{2}\right\}\left\{m\left(l_{CG} + \frac{d}{2\tan\bar{\theta}_a}\right)^2 + I_{CG}\right\}^{-1} \quad (1)$$

From the above equation, the condition for the pendulum motion is as follows:

$$\frac{d^2}{4a\cos\bar{\theta}_a}\left(\frac{1}{\tan^2\bar{\theta}_a} + 1\right) + \frac{d\tan\bar{\theta}_a}{2} > l_{CG} \quad (2)$$

Given that the distance between the CG and the wire position can be increased further when there are fixing devices at the upper and lower parts, the condition listed above can be used as a conservative design criterion for the stability of the wind turbine.

2.4. Validation of Analytic Approach Based a Small Model Test

To verify the theoretical analysis method, the theoretical results were compared with the numerical results calculated using Simulink in MATLAB (r2016a, MathWorks, Natick, MA, USA) and the test results of the simplified small model. To simulate the pendulum motion of a bar whose CG is different from its geometric center, a simple small model was used which consisted of a pipe fixed using an aluminum frame with a closed end to which an additional mass was attached. To realize the motion of a two-dimensional pendulum connected to two rigid wires of the same length, the wires were replaced with rods with bearings. Figure 11 shows the conceptual diagram of the simplified model, and Figure 12 shows the simple model used for testing. This two-dimensional simplified model shows 1-degree-of-freedom (DOF) motion according to Kutzbach's equation in Equation (3) [8].

$$M = 3(L - 1) - 2J_1 - J_2 \quad (3)$$

where M denotes the DOF, L is the number of links with the ground, J_1 is the number of full joints, and J_2 is the number of half joints. The experiment was performed for three cases with different weights of the upper dummy mass, and the natural frequency was measured based on a frequency analysis (fast Fourier transform (FFT)) of the displacement signal of the specimen. As shown in Figure 12, a noncontact type laser sensor was used for displacement measurement so that the sensor attachment did not act as a disturbance to the test target.

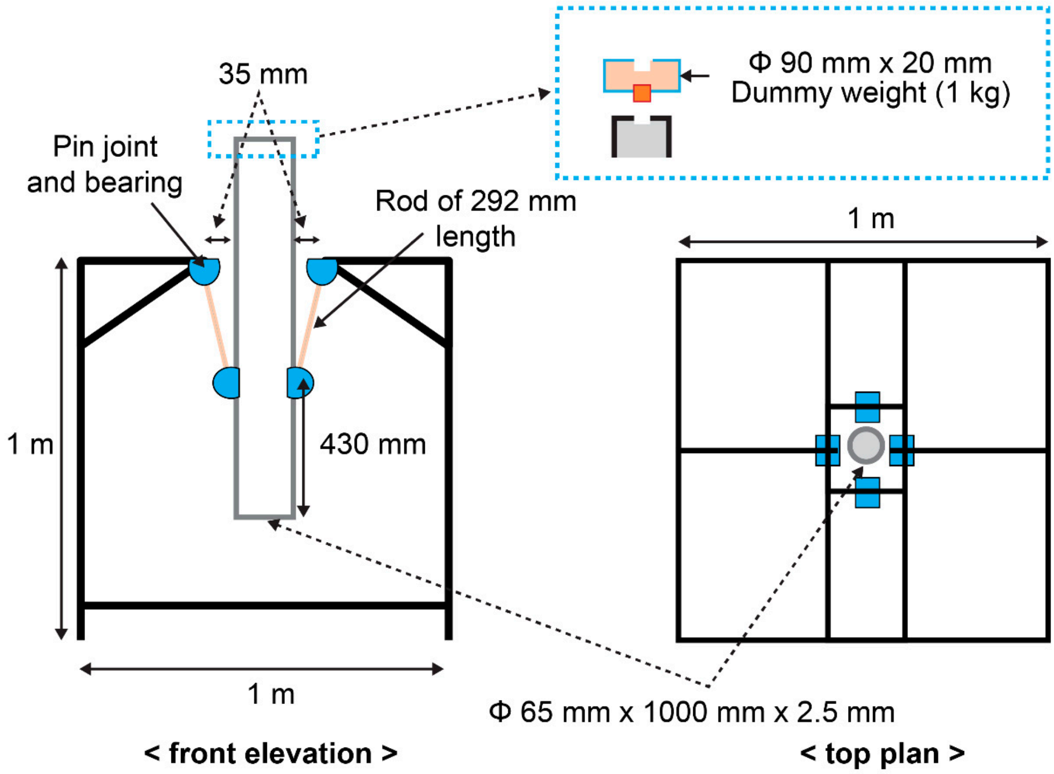

Figure 11. Specifications of simple model.

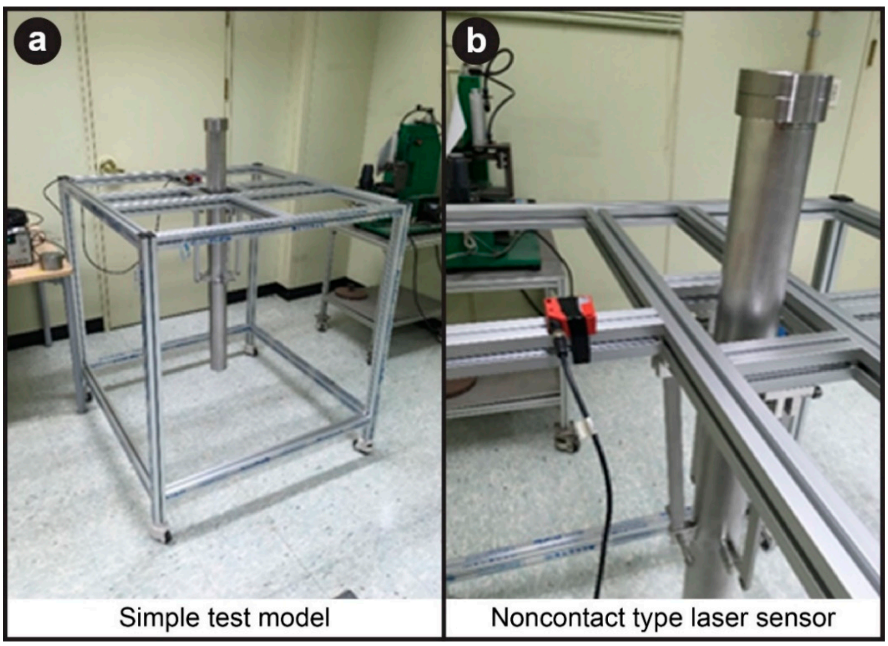

Figure 12. Measurement of natural frequency with a simple test model.

For additional verification of the theoretical model, a numerical analysis model for simulating the behavior of a wind turbine was constructed and utilized using Simulink. Figure 13 shows the model used in Simulink for analysis. To simulate the simple model shown in Figure 12, the analysis models of the wind turbine structure, rigid rod (link), and hinge (pin) were constructed using the rigid model. The size and position of the rigid rod and the position of the hinge were modeled in detail with the actual design value of the simple model. The detailed model of the structure was also modeled in consideration of the structure's shape and weight, and the position of the hinge. All elements used were rigid and did not deform when forces were applied. The numerical model calculates the response of the structure (the movement of the wind turbine) from the equation of motion of the entire system. The natural frequency of the structure can be obtained based on the FFT of the calculated response or by measuring its period.

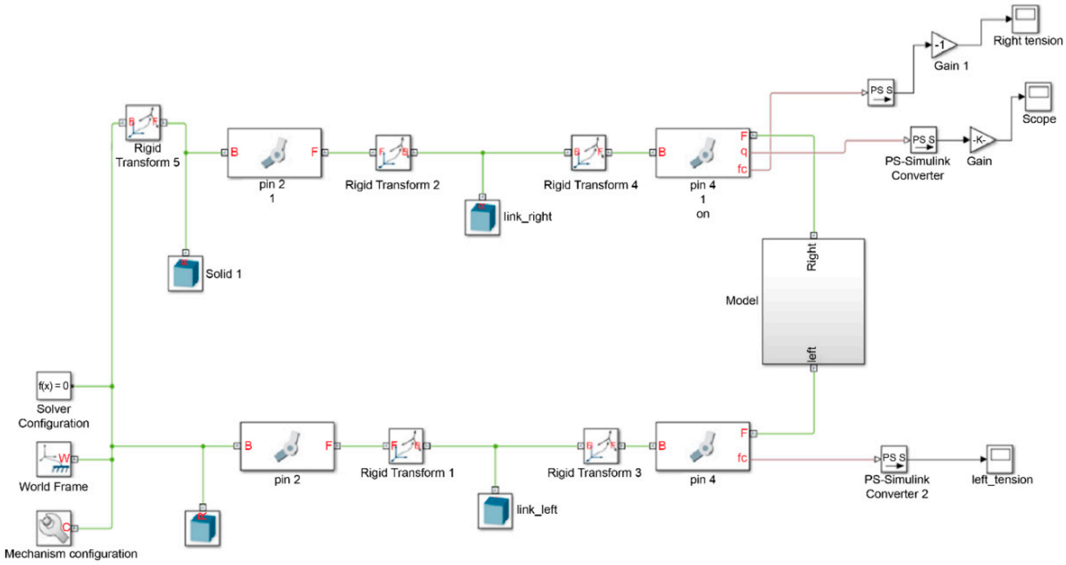

Figure 13. Simulink model used for numerical analysis.

Table 1 shows the change in natural frequency at increasing dummy weights and compares the natural frequencies calculated through the theoretical and numerical analysis of the simple model with the experimental results. The difference among theoretical, numerical, and experimental results is due to the assumption of very small angular change in the theoretical analysis, uncertainty of the position of the CG of the test model, and influence of damping in joints and bearings. However, since the difference is sufficiently small, the design condition (Equation (2)) derived by the theoretical analysis can be used as a conservative design criterion for the stability of the wind turbine.

Table 1. Natural frequency based on theoretical analysis.

l_{wt} (m)	1	1	1
d (m)	0.122	0.122	0.122
a (m)	0.292	0.292	0.292
l_{CG} (m)	0.07	0.07	0.07
$\overline{\theta}_a$ (°)	6.67	6.67	6.67
m (kg)	5.83	5.83	5.83
Dummy weight (kg)	0	1	2

Table 1. *Cont.*

Natural frequency (Hz)	Theoretical model	0.71	0.60	0.53
	Numerical model	0.71	0.61	0.54
	Experiment	0.72	0.62	0.56

3. Structural Design and Fabrication of the MMB

In this section, major design variables, such as operating conditions, working environment, application depth, and the target turbine of the MMB are presented, and the final design and manufacturing process are described. First, given that the purpose of manufacturing the MMB is to install offshore wind turbines onsite within a single day, the sea state of operation conditions was classified as Seastate 3, which is relatively mild. In addition, by limiting the operation area to the inshore zone to cover most of the domestic offshore wind farm construction areas, the various legal restrictions and external force conditions (significant wave height with a frequency of 20 years, etc.) are mitigated. This minimizes the size and manufacturing cost of the vessel. Regarding the applied depth, priority was given to areas within 20 m of the developed wind farm. In particular, in the case of the target turbine, which is a determinant of the ship's specifications, and the lifting capacity of the A-Frame, a 4.2 MW product with the largest capacity among domestic offshore wind turbines and a blade diameter of 136 m was selected from Uinson (Daejeon, Korea). Table 2 contains a summary of the data.

Table 2. Operating condition of multipurpose mobile base.

Category	Sea State	Water Depth	Current Speed	Wind Speed	Wind Turbine	Working Sea Area
details	3	<20 m	<1.2 m/s	<8 m/s	4.2 MW, D136 m	inshore zone

Following the examination of various types of lifting methods based on the above conditions, a lifting method using mainly wires and clamping devices was derived, and the final MMB design was confirmed in the form of a crane barge equipped with an A-Frame. Subsequently, in accordance with the ship design regulations of the Korean Register of Shipping, a direct global structural analysis and motional analysis for the hull and A-frame, calculation of the ultimate design wave based on probability statistics, and mooring analysis were performed. Figure 14 shows the final design of MMB.

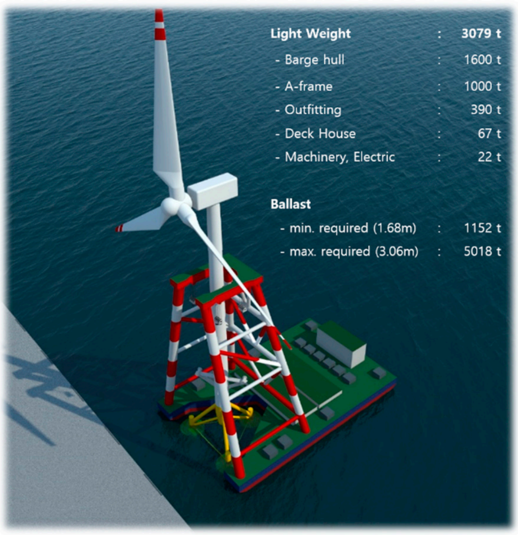

Figure 14. Final design of multipurpose mobile base (MMB).

3.1. Suction Bucket Uplift Analysis

This section deals with the technical prerequisites for the A.I.O.I of an offshore wind turbine, namely, the process of calculating the required pull-out pressure of the suction bucket foundation to separate the entire turbine system temporarily assembled from the seabed at the port and measuring the inclination of MMB and tower to ensure safety. The results of the CPT investigation of the ground in the port where the temporary turbine assembly was made are shown in Figure 15.

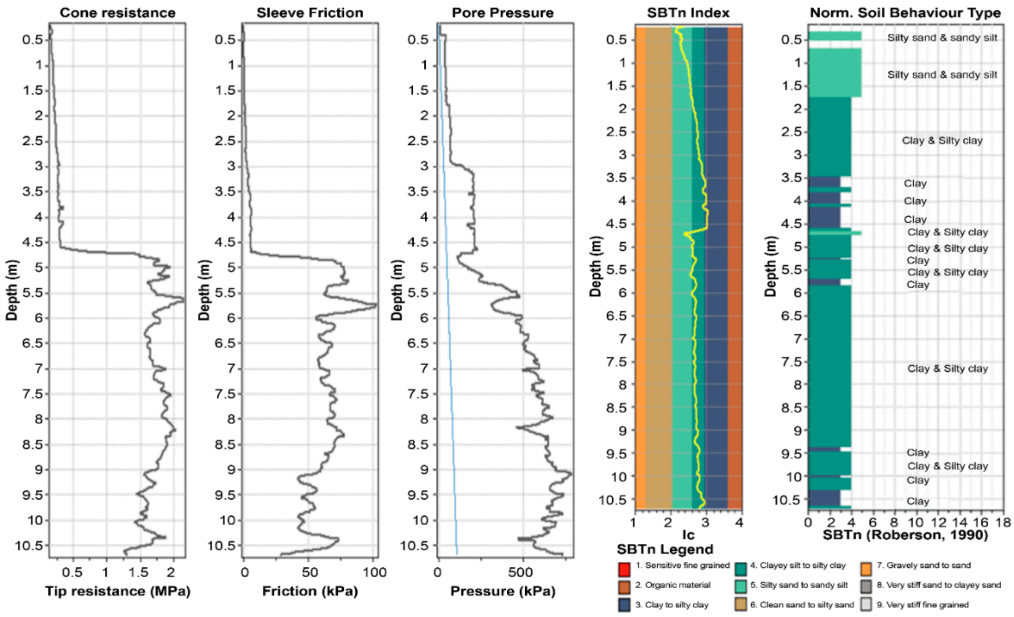

Figure 15. Test results of cone penetration of port (source: CPT-based SBTn chart suggested by Robertson, 1990).

Based on the results presented in Figure 15, the design parameters of the ground were calculated by dividing the soil in two layers as shown in Table 3. The value obtained at this time is conservative, similar to the examination of the bearing capacity of the suction bucket, which does not apply the material factors for the corrosion thickness and ground properties of the foundation.

Table 3. Soil parameters of port.

Depth (m)	Soil	N Value	Unit Density (kg/m^3)	Undrained Shear Strength (kPa)
0.2–4.5	clay	1/30	17.5	15.5
4.5–10.7		7/30	17.5	105.9

The self-weight of the offshore wind turbine system, including the suction bucket, was calculated as the design weight with the addition of 5% to the net weight, and the required pull-out resistance of the suction bucket was calculated using the Suction Pile Loading Capacity Calculation Program (SPLC), a suction bucket bearing capacity analysis program developed by the South Dakota School of Mines and Technology [9]. Table 4 shows the input conditions for the design analysis of the SPLC.

Table 4. Design parameters for the SPLC.

Category		Design Value
Pile parameters	length	9.3 m
	diameter	8.0 m
	wall thickness	20 mm
	cap thickness	25 mm
Hydraulic condition	water depth	10 m
	unit weight of water	10.1 kN/m^3
Loading condition	suction bucket under water weight	2461 kN/each

As a result of the calculation of the pull-out resistance for each suction bucket when the turbine system is pulled out according to the aforementioned conditions, the maximum pulling force was calculated to be 17,534 kN. Dividing this by the area of the suction bucket top plate (50.26 m^2) with a diameter of 8 m, the minimum pressure inside the suction bucket was calculated as 348.9 kPa. At this time, as the maximum pressurization capacity of the pump system used for pulling out was 1200 kPa, and the required pull-out force could be secured.

3.2. Fabrication of the MMB

In this section, we will explain the manufacturing process of the MMB, a special ship for the A.I.O.I of offshore wind turbines. Given that the manufacturing of the MMB is not the main research content of this project, only a brief overview of the manufacturing process will be included. The MMB was manufactured by separately manufacturing and assembling the lower hull and upper A-Frame. A closing bar was installed to close the opening at the top of the A-Frame and to increase structural stability by reducing the displacement of the area wherein stress was concentrated. In addition, a clamping device was added to the A-Frame to prevent shaking and overturning of the structure during transportation. In particular, a support beam, which was not reflected in the initial design, was added. As this is a device used to set down and fix the entire wind power system lifted by the wire, and was manufactured and installed at the request of the ship certification body, it is necessary to comply with the maritime law that states that all cargo transported by sea should be fastened to the ship and transported with 6-DOF restrains [10].

Therefore, these requirements have been fulfilled and the concepts mentioned are summarized in Figure 16. Figure 17 shows the manufacturing process of the MMB.

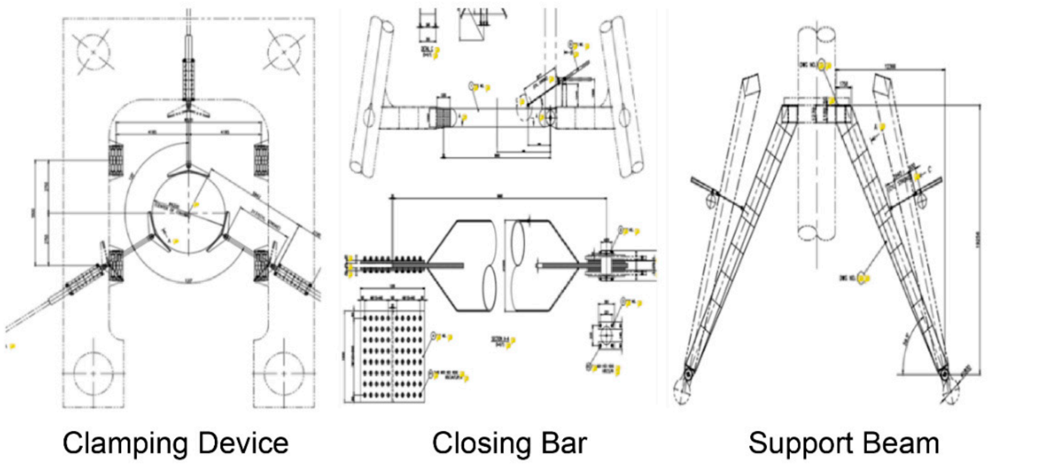

Figure 16. Auxiliary devices of the MMB.

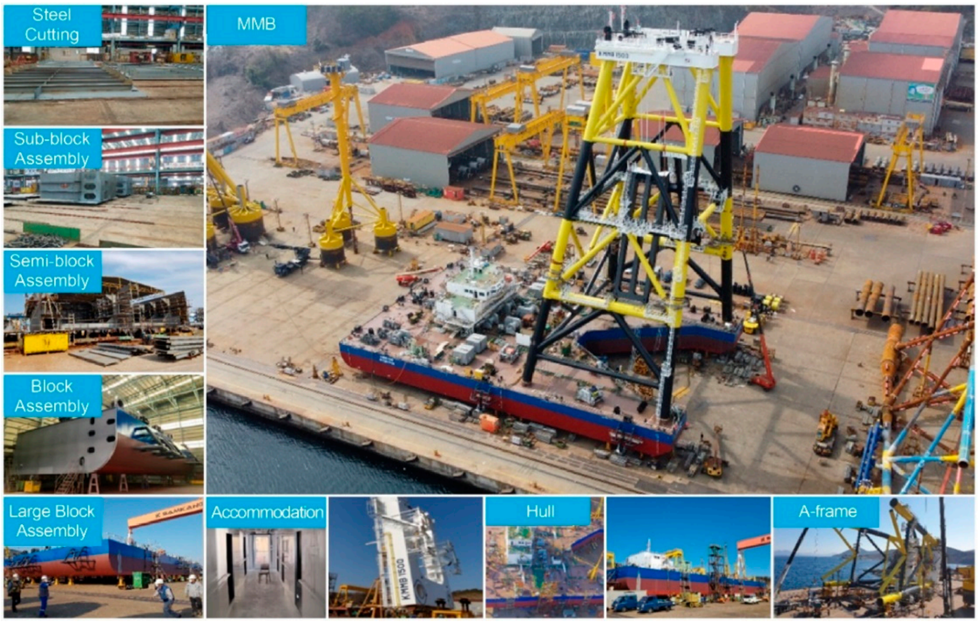

Figure 17. Fabrication of the MMB.

4. Field Test and Performance Evaluation

4.1. Measurement Configuration

The MMB, manufactured for the A.I.O.I of offshore wind turbines, transports the entire turbine system, including the lower foundation at once. Thus, securing stability during operation is of upmost importance. To evaluate stability, inclination sensors were attached to the body, tower, and A-Frame of the MMB. The inclination sensors (HCA520T-10, resolution 0.001°, absolute accuracy 0.005°) attached to the hull were capable of high-sensitivity inclination measurements along two axes (roll/pitch). The same type of inclination sensors were also applied at three points (top, middle, bottom) of the tower to measure the upward, downward, left, and right movements of the wind turbine assembly. In addition, noncontact laser sensors (A, B, C) were installed to measure the displacement of the wind turbine in the translation direction at the top of the A-Frame. Figure 18 shows the locations of the installed sensors.

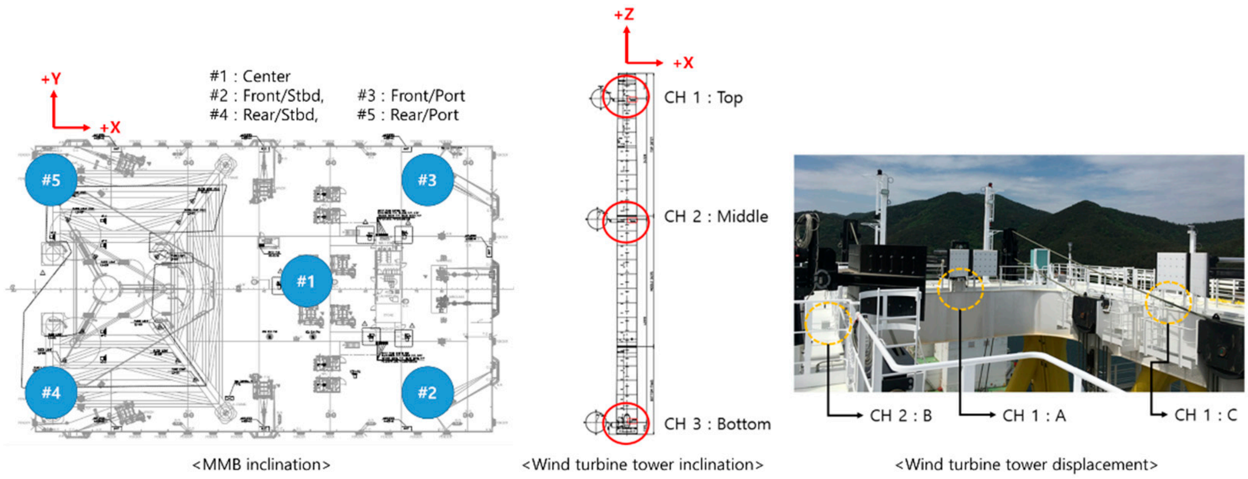

Figure 18. Measurement configuration of the MMB.

4.2. Measurement Conditions

To measure the behavior of the MMB and wind turbine assembly, five measurements were conducted, as listed in Table 5. Case 1 was conducted while moving to the demonstration site after the MMB was manufactured, and only the inclination of the MMB was measured in a situation in which the wind turbine assembly was not loaded. Case 2 was implemented while the wind turbine assembly was loaded on the MMB, and the support beam was fully fastened while sailing in the inner harbor. Case 3 was implemented when the wind power generator assembly was loaded on the MMB that was anchored at the port, and was measured in very bad weather conditions. Cases 4 and 5 were conducted in actual field demonstration conditions. In Case 4, the wind turbine assembly was lifted, transported to the MMB in the loading state, and then transported to the installation site. In Case 5, the entire wind turbine assembly was lowered after arriving at the installation site and placed at the target location.

Table 5. Measurement condition of the MMB.

Category	Date in 2021	Operation Condition	Operation Time	Seastate
case 1	12–13 May	sailing without (w/o) wind turbine	20 h	2~3
case 2	2 July	sailing with (w/) wind turbine	4 h	2
case 3	4 July	mooring w/wind turbine	13 h	3
case 4	9 July	sailing w/wind turbine	4 h	2
case 5	9 July	lowering of wind turbine	6 h	2

4.3. Field Test and Results

Figure 19 shows the inclination measurement results for Case 1 conducted during the self-operation of the MMB in the absence of a wind turbine assembly. In the figure, the MMB was anchored in the nearby sea until 12:00 on 12 May, and the result after that shows the behavior during sailing. Although the inclination at the fifth measurement point appears slightly different due to local deformation at each location, the value at the center position can be used as a representative value for the behavior of the entire hull. The slope at the center is less than 0.3° in the root-mean-square (RMS) value (Figure 19a,b) and less than 2° in the peak-to-peak value (Figure 19c,d). This indicates that the MMB has sailed stably.

Figure 20 represents three-dimensional diagrams of the spectrum of the slope measured at the center of the MMB. In the figure, it can be seen that the main frequency of behavior during MMB operation is around 1 rad/s in the X and Y directions, and the other frequency components are very small. These dominant frequency components are in close agreement with the ocean wave period data (Figure 21). Accordingly, it can be said that the behavior of the MMB is affected primarily by the wave.

In Case 2, the MMB was operated in the inner harbor with the wind turbine assembly loaded. As shown in Figure 22, the behavior of the MMB is smaller than that in Case 1 because the stability was increased by the weight of the assembly. Based on this, the success possibility of A.I.O.I in which the entire wind turbine was lifted and installed at once was confirmed.

In Case 3, the MMB was moored at the port with the wind turbine assembly loaded, and subjected to increased external force (waves and wind) due to bad weather. Owing to the influence of the high wave height, the inclination of the MMB changes up to 0.3° in the RMS value in the Y direction and up to 2.5° in the peak-to-peak value, as shown in Figure 23. Although the wind turbine tower can undergo motion with increased inclinations (peak values up to 6° in Figure 24) compared with that of the MMB owing to its flexibility, it is judged that there is not a major problem in safety as long as the stress does not exceed the design value from a structural point-of-view.

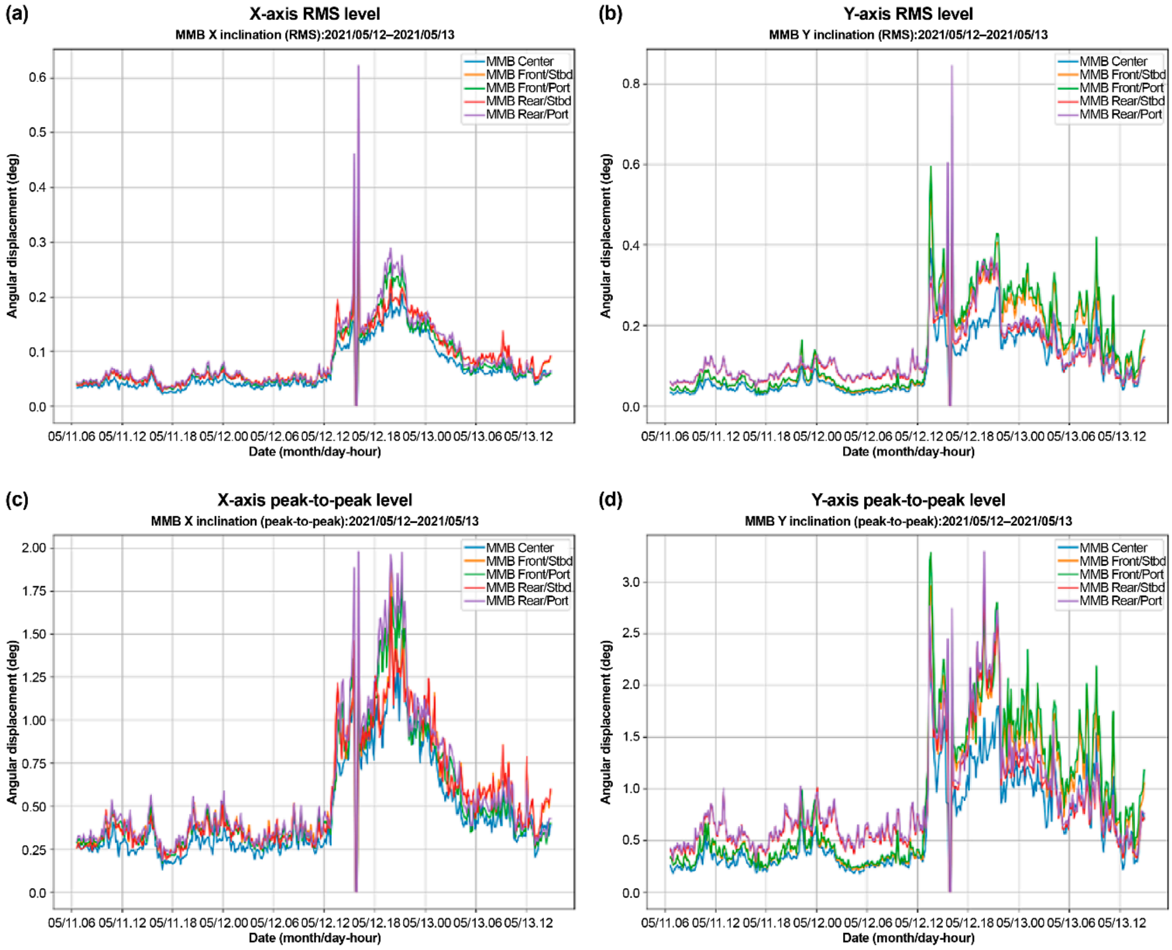

Figure 19. Inclination of the MMB in Case 1.

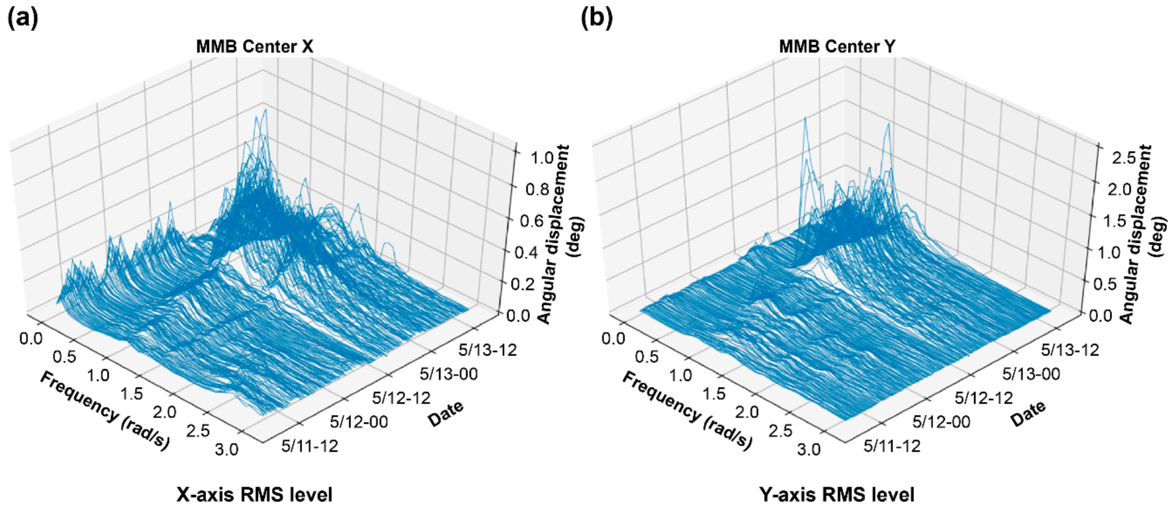

Figure 20. Waterfall chart of the center position inclination of the MMB in Case 1.

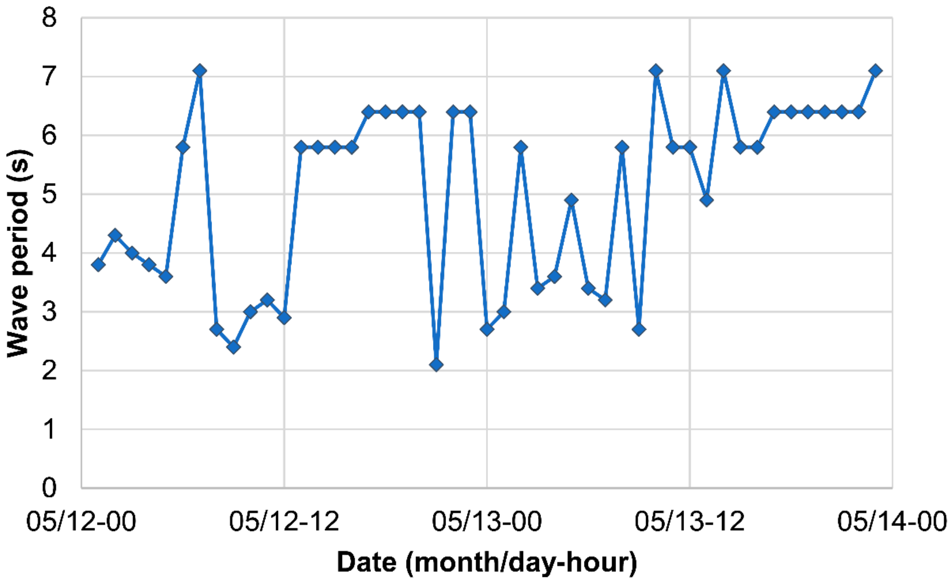

Figure 21. Wave period during Case 1.

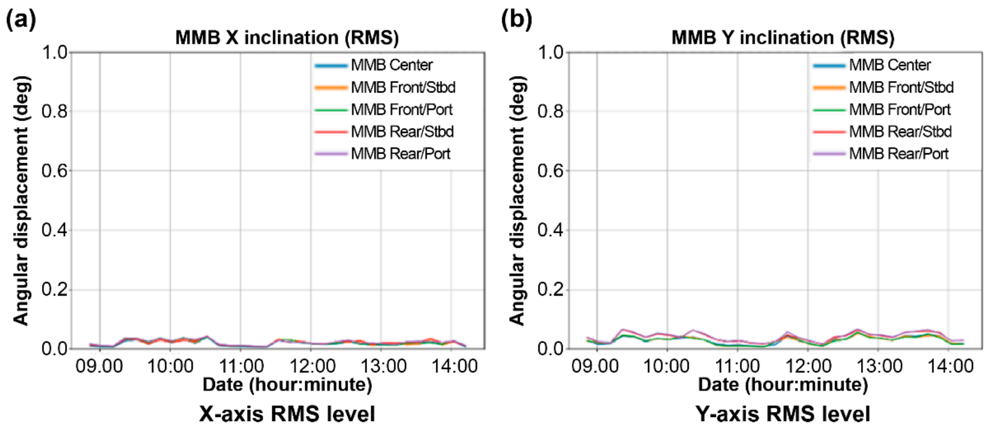

Figure 22. Inclination of the MMB in Case 2.

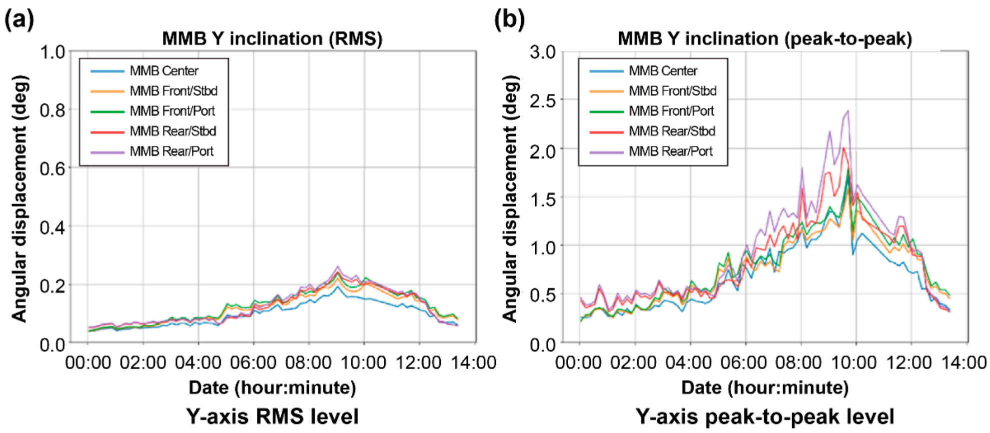

Figure 23. Inclination of the MMB in Case 3.

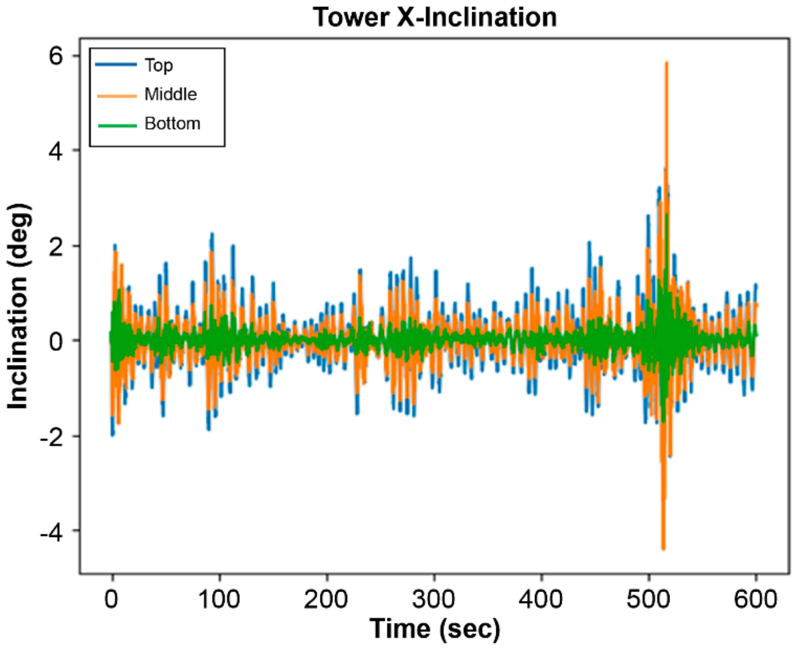

Figure 24. Inclination of wind turbine tower in Case 3.

Cases 4 and 5 are the field demonstration process for the A.I.O.I of an offshore wind turbine by the MMB as shown in Figure 25, and include operations in the open sea as well as the inner port. Therefore, the slope change in Cases 4 and 5 may increase compared to that in Case 2.

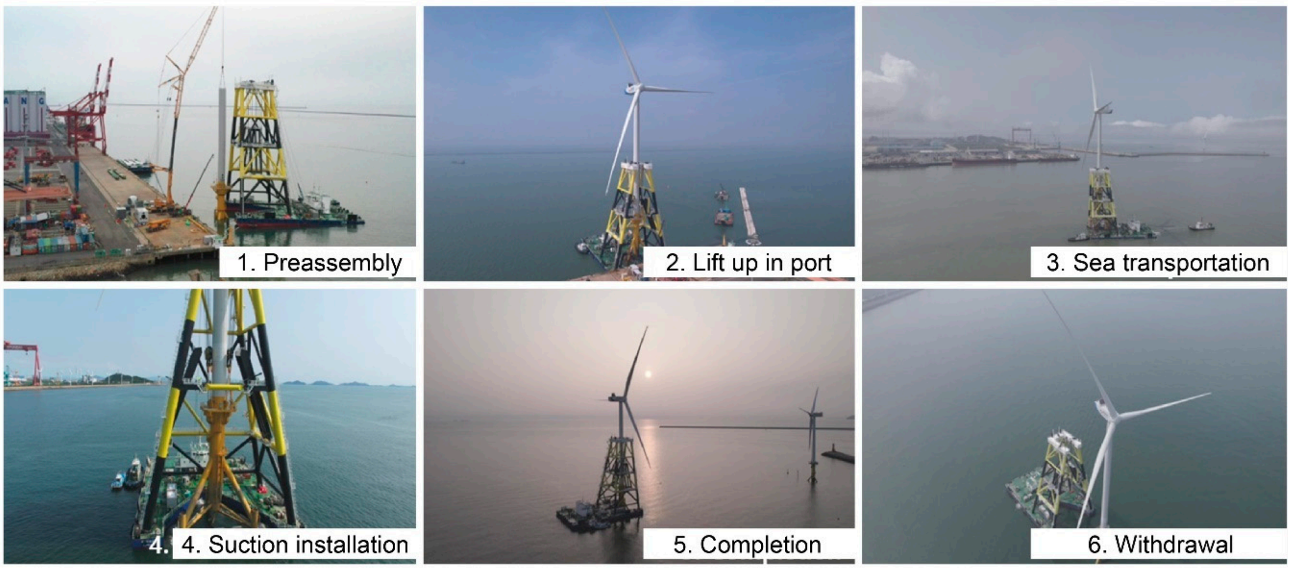

Figure 25. AIOI of offshore wind turbine by the MMB.

Figure 26 shows that in Case 4, the inclination of the MMB in the X and Y directions changed approximately 0.1°, and the slope change of the wind turbine tower was approximately 0.2°, so that the all-in-one transportation of the offshore wind turbine was performed very stably.

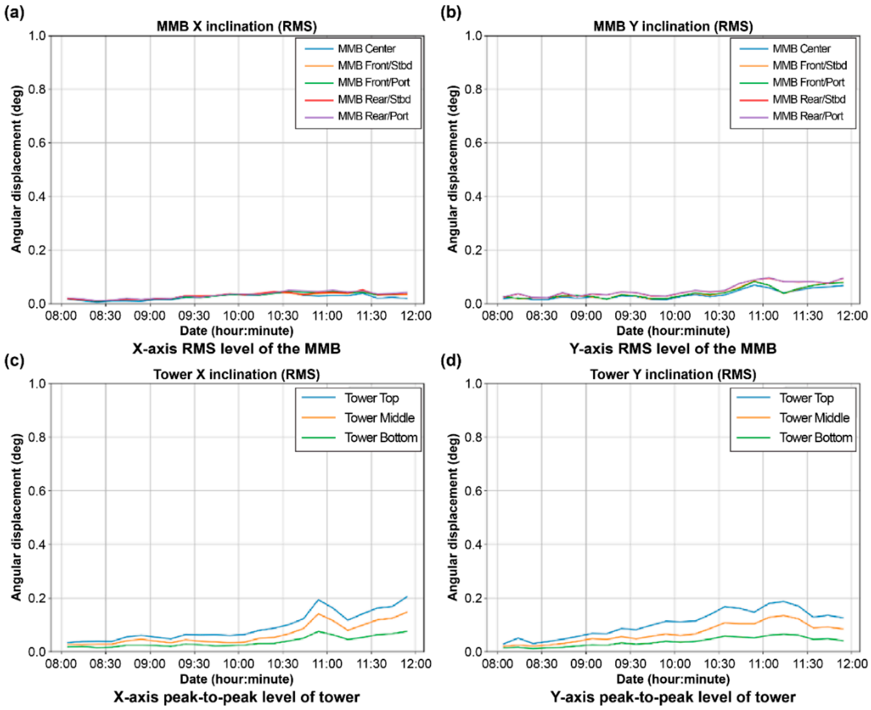

Figure 26. Inclinations of the MMB and tower in Case 4.

In Case 5 (Figure 27), the inclinations of the MMB and the wind turbine tower were measured while the entire wind turbine assembly was lowered after arriving at the installation site and placed at the target location. In the figure, it can be observed that the slope of the tower increases significantly at the moment when the suction bucket touches down on the seabed (approximately 16:30) and then decreases rapidly thereafter. This is because the load applied to the MMB moves to the foundation of the suction bucket after the wind turbine is seated on the seabed. The small slope change in Cases 4 and 5 proves that the A.I.O.I of the offshore wind turbine is a very stable installation method.

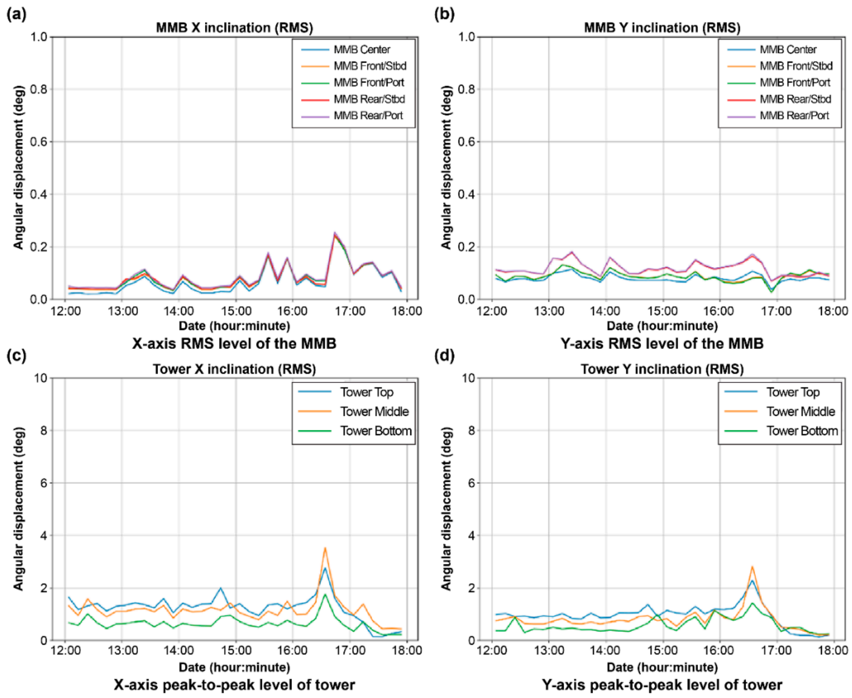

Figure 27. Inclinations of the MMB and tower in Case 5.

5. Conclusions

This study developed an innovative offshore wind turbine single-day installation method that lifts the wind turbine system with the support structures, transports it by sea, and then installs it in the sea using the suction method. The following conclusions were drawn by the development of a stable analysis technique and successful field demonstration of A.I.O.I with a full-scale offshore wind turbine.

1. A two-dimensional analysis model was developed for the assembly in which the wind turbine and the support structure were combined, and the condition of the vertical distance between the wire connection point and the CG of the wind turbine required to prevent overturning during hoisting/unloading of the wind turbine was presented according to Equation (2). Based on the analysis, it is possible to control sudden changes in the MMB behavior because the location of the wire connection point can be calculated in consideration of the operating range (moving distance between the top and bottom) when the wind turbine is hoisted using the MMB.
2. To verify the two-dimensional wind turbine behavior analysis method, a scaled-down model was prepared and tested, and the analysis method was verified based on its comparison with the theoretically predicted result. Moreover, additional verification was performed with the use of the SPLC, and the accuracy of the technique was verified based on the intercomparison of the results. The natural frequency calculation result of the two-dimensional analysis model, the theoretical analysis result of 0.72 Hz, the numerical analysis model at 0.71 Hz, and the scaled model field test at 0.72 Hz, confirmed that the theoretical formula, the test result, and the rigid body analysis result obtained by the commercial program agreed closely.
3. Field demonstration was conducted for an actual 4.2 MW commercial turbine, and the dynamic behaviors of the MMB and wind tower were recorded by the measurement system. The following conclusions were obtained. It was confirmed that the main frequency component of the dynamic behavior of the MMB in the no-load state (without the wind turbine assembly) was almost consistent with the periodic data of ocean waves. In addition, the behavior of the MMB when the wind turbine assembly was mounted was not very different to the no-load state for both the hull and the tower. In the actual A.I.O.I demonstration test, very stable values were obtained. The respective changes in inclination at the center of the MMB and the tower were within 0.1° and 0.2° during operation because of the reduction of longitudinal and transverse sway of the MMB induced by the self-weight assembly and ballast.

In conclusion, the technical stability of the MMB achieved through this project is quite high. Accordingly, it can be inferred that it is a meaningful project that successfully demonstrated, to our knowledge, for the first time the single-day installation feasibility of offshore wind turbines onsite. In the future, additional research will be conducted for the improvement of the clamping device developed herein, and the advancement of the real-time verticality control model for the wind turbine assembly using the hydraulic system.

6. Patents

Lateral Displacement Hydraulic Control Device For Up-right Offshore Transportation Of High Slenderness Ratio Heavy Structure Such As Offshore Wind Turbine (P2019-1254-KR).

Author Contributions: Conceptualization and Methodology, M.-S.R. and S.-R.K.; Formal analysis, M.-S.R. and D.-H.C.; Investigation, M.-S.R.; Resources, M.-S.R. and D.-H.C.; Data curation, M.-S.R. and J.-G.K.; Validation, M.-S.R., S.-R.K. and J.-G.K.; Writing—original draft preparation, M.-S.R.; Writing—review and editing, S.-R.K. and D.-H.C.; Funding acquisition, M.-S.R. All authors have read and agreed to the published version of the manuscript.

Funding: This research was supported by Korea Electric Power Corporation Research Institute (KEPRI).

Institutional Review Board Statement: Not applicable.

Informed Consent Statement: Not applicable.

Data Availability Statement: Not applicable.

Acknowledgments: This work was supported by Ministry of Oceans and Fisheries Gunsan Regional Office.

Conflicts of Interest: The authors declare no conflict of interest.

References and Notes

1. Global Wind Energy Council. *Global Wind Report 2022*; Global Wind Energy Council: Brussels, Belgium, 2022.
2. European Environment Agency. *Europe's Onshore and Offshore Wind Energy Potential: An Assessment of Environmental and Economic Constraints*; EEA Technical Report No. 6; European Environment Agency: Copenhagen, Denmark, 2009.
3. Ryu, M.; Lee, J.; Kwag, D.; Seo, Y. Verification of tripod suction pile applicability through dynamic characteristic analysis of offshore wind turbine at each installation stage. *J. Korea Wind Energy Assoc.* **2019**, *10*, 12–21.
4. Ryu, M.; Jung, M.; Lee, J.; Kim, D. Closed form solutions for predicting lateral response of tripod suction pile for offshore wind turbine foundation. *Energies* **2020**, *13*, 6176. [CrossRef]
5. Seo, Y.; Ryu, M.; Oh, K. Dynamic characteristics of an offshore wind turbine with tripod suction buckets via full-scale testing. *Complexity* **2020**, *2020*, 3079308. [CrossRef]
6. Webinar: An offshore wind vessel and other O&G sector opportunities, Clean Energy Group, 6 June 2017.
7. Korea wind energy industry association, 2020.
8. Norton, R.R. *Design of Machinery*; McGraw-Hill: New York, NY, USA, 1999.
9. Bang, S.; Cho, Y. Suction pile loading capacity evaluation program, 2006.
10. Ministry of Oceans and Fisheries. *Standard of the Structure and Equipments for Barge Ships (Article 28)*; Notification of Ministry of Oceans and Fisheries 2020–109; Ministry of Oceans and Fisheries: Sejong City, Korea, 2020. (In Korean)